Identification of an Isoaspartyl Linkage Formed upon Deamidation of Bovine Calbindin D_{9k} and Structural Characterization by 2D ^1H NMR†

Walter J. Chazin,*,‡ Johan Kördel,‡,§ Eva Thulin,§ Theo Hofmann,§,∥ Torbjörn Drakenberg,§ and Sture Forsén*,§

Department of Molecular Biology, Research Institute of Scripps Clinic, 10666 North Torrey Pines Road, La Jolla, California 92037, and Department of Physical Chemistry 2, Chemical Center, Lund University, P.O. Box 124, S-22100 Lund, Sweden

Received February 27, 1989; Revised Manuscript Received June 26, 1989

ABSTRACT: Preparations of recombinant bovine calbindin D_{9k} (r-calbindin) that appear homogeneous on SDS electrophoresis gels have been shown by isoelectric focusing to be mixtures of proteins differing in net charge. The production of two isoforms with increased negative charge occurs during a routine urea denaturation step and can be effectively suppressed by replacing this procedure with thermal denaturation. The two isoforms have been separated from the native protein by DEAE-Sephacel ion-exchange chromatography. Amino acid sequencing of tryptic peptide fragments and two-dimensional (2D) ^1H NMR studies establish that the isoforms correspond to calbindin D_{9k} deamidated at Asn56 and that the major product has an isoaspartate (β-linked peptide) residue at this position. The minor deamidated component is found to have a normal Asp-Gly α-linkage. A detailed analysis of proton chemical shifts, ϕ backbone dihedral angles, and nuclear Overhauser effects indicates that the global conformation of r-calbindin is not perturbed upon deamidation and that all elements of secondary structure are intact. The Asp56 form is nearly identical with the intact protein, whereas the structure of the iso-Asp56 form is perturbed, predominantly in the polypeptide segment Lys55–Asp58. These studies demonstrate that 2D ^1H NMR techniques can be used to identify and quantitate the two isoforms produced upon deamidation of a protein and to assess changes in the local and global conformation.

Deamidation appears to be one of the most common nonenzymatic modifications of proteins (Gracy, 1983; Harding, 1985; Ahern & Klibanov, 1987; Yüksel & Gracy, 1986). At the present time little is known about the circumstances under which the reaction occurs or of its possible biological consequences. Deamidation in vitro, as a result of drastic treatments during protein isolation and purification or of prolonged storage of proteins at elevated temperatures, is well documented. However, evidence is accumulating that deamidation also occurs in vivo (DiDonato et al., 1986; Aswad & Johnson, 1987; Geiger & Clarke, 1987; Johnson et al., 1987). Deamidation has been suggested to be an initial step in the catabolism of at least some mammalian proteins and to represent a biological clock related to aging (Gracy, 1983; Robinson & Rudd, 1987). To mention just a few examples, deamidated forms of the protein α-crystalline accumulate in old cells in the center of the eye lens (Ikeda & Sawano, 1971), and similarly deamidated forms of triosephosphate isomerase (TPI) are observed in many types of aging cells, from skin fibroblasts of old donors (Tollefsbol & Gracy, 1983) to old red blood cells (Turner et al., 1975). The phenomenon of deamidation does not seem to be restricted to mammals. It has also been observed in *Drosophila* (Robinson, 1979).

A particularly important aspect of deamidation, and one that has recently attracted considerable attention, is the likely formation of isopeptide linkages (sometimes referred to as β-peptide linkages) when an asparagine is followed by a glycine in the sequence. Deamidation of the Asn-Gly linkage primarily takes place via a cyclic imide intermediate (Figure 1) that may open up in two different ways: either to form a normal Asp-Gly peptide linkage (A) or to form an isoaspartyl linkage (B) (Bornstein, 1970; Bornstein & Balian, 1970). The isopeptide form may in fact be the most favored product—yields of between 70 and 85% have been observed in some naturally occurring and synthetic model peptides (Aswad & Johnson, 1987; Meinwald et al., 1986; McFadden & Clarke, 1987).

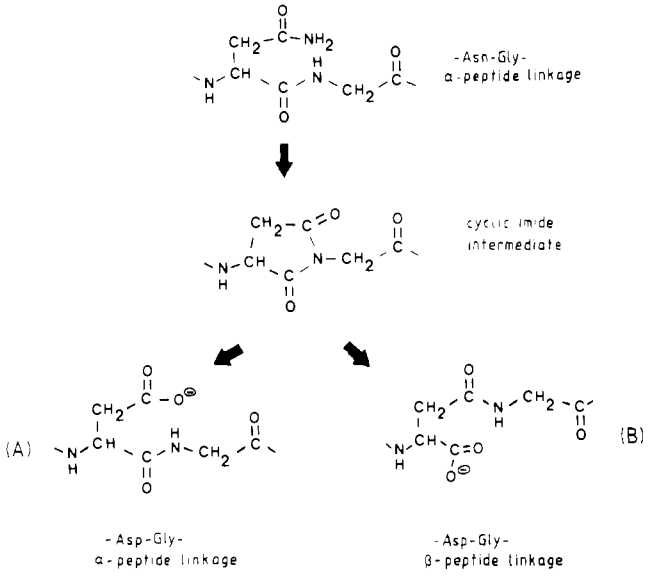

FIGURE 1: Schematic routes of deamidation of Asn-Gly peptide linkages. Through intramolecular nucleophilic substitution a cyclic imide intermediate may form. The cyclic imide may open at either of the two C–N bonds to form a normal Asp-Gly linkage (A) or an isoaspartyl linkage (B) [after Bornstein and Balian (1970)].

† This work was supported by a grant from the National Institutes of Health (GM 40120, to W.J.C.) and by a graduate fellowship (to J.K.) and operating grants (to S.F. and T.D.) from the Swedish Natural Science Research Council.

* To whom correspondence should be addressed.
‡ Research Institute of Scripps Clinic.
§ Lund University.
∥ On leave from the Department of Biochemistry, University of Toronto, Canada.

0006-2960/89/0428-8646$01.50/0

The α-carboxylate group at isoaspartyl linkages has recently been shown to be specifically methylated by eucaryotic carboxyl methyl transferases (Aswad & Johnson, 1987; Clarke, 1985). The biological role of this enzymatic methylation is poorly understood. The reaction has been considered to represent the first step in a repair process that leads to the reversal of the deamidation (Aswad & Johnson, 1987; Clarke, 1985; Johnson et al., 1987). Methylation has also been considered a trigger of further catabolic reactions of the transformed protein. There remains also a possibility that the methyl transferases may play a role in the regulation of protein function (Aswad & Johnson, 1987; Clarke, 1985).

Deamidation of a protein or peptide introduces new negative charges that may influence tertiary structure and stability. However, the structural and functional consequences of deamidation may differ from protein to protein. In the case of the mouse epidermal growth factor, deamidated forms of the polypeptide have almost the same mitogenic activity as the intact form (DiAugustine et al., 1987). In contrast, in the dimeric enzyme TPI, deamidation introduces new negative charges at subunit contact surfaces, which increases subunit dissociation and thermal lability (Yüksel & Gracy, 1986). When an isoaspartyl peptide linkage is formed, an additional CH_2 group is introduced into the main chain, which could conceivably cause considerable perturbation of normal secondary and tertiary protein structure. No experimental study as to the occurrence and extent of such structural changes in proteins is, however, yet available. In this paper we show that current 2D[1] ^1H NMR techniques permit the unambiguous determination of a site of deamidation and the presence of an isoaspartyl linkage (as well as of a normal Asp-Gly linkage) in bovine calbindin D_{9k},[2] a Ca^{2+} binding protein of 75 amino acids. The site of deamidation is found to be Asn56, which is followed by a glycine residue and situated in the Ca^{2+}-binding loop of the C-terminal calcium site.

The purification procedures used to isolate recombinant bovine calbindin D_{9k} expressed in *Escherichia coli* have been described in detail (Brodin et al., 1986). The purity of the proteins produced was established by migration as a single band on SDS–PAGE and agarose gels and by one-dimensional ^1H NMR (obtained at 360 MHz) showing a number of resolved resonances with no trace of impurity peaks. Recently, these analytical techniques have been complemented with isoelectric focusing (IEF) to achieve a more powerful purity characterization. It then became evident that some protein preparations previously regarded as pure and homogeneous in fact were mixtures of two or three isoforms that migrated at different rates on the IEF gels and, therefore, represented forms of r-calbindin differing in net charge.

At about the same time 2D ^1H NMR studies at 500 MHz of wild-type recombinant bovine calbindin D_{9k} (r-calbindin) were initiated. In some of the initial COSY and NOESY experiments extra peaks were present in some spectral regions that could be best explained as arising from one or more isoforms of the protein. These were clearly not related to the previously documented cis–trans isomerization at Pro43 (Chazin et al., 1989). The number of extra peaks is small as are the chemical shift differences from the probable parent signals. This implies that the solution tertiary structure of the intact r-calbindin and those of the isoforms are very similar. Moreover, the relative intensities of parent and "satellite" NMR signals roughly agreed with the relative amount of the different isoforms as observed through IEF studies. To identify the molecular basis of the isoforms, which we presumed to be the result of deamidation, we separated the isoforms by chromatographic methods and also carried out an in-depth 2D ^1H NMR analysis on the mixture of isoforms.

Materials and Methods

Protein Isolation and Sequencing. Samples containing mixtures of isoforms of wild-type or the M2 mutant (used only for protein sequencing, see below) r-calbindin were obtained as described previously (Brodin et al., 1986; Linse et al., 1987). Separation of isoforms was achieved as follows. Suspended pellets from a 10-L fermentation of *E. coli* expressing wild-type r-calbindin were treated as described earlier (Brodin et al., 1986; Linse et al., 1987) up to the point where the solutions were passed through a Pharmacia G-50 column, which was the last step in the original purification procedure. The pooled r-calbindin fractions obtained after the Sephadex G-50 column in 50 mM ammonium acetate buffer, pH 6.0, were made 3 mM in EDTA and brought to pH 7.5 through the addition of Tris. This solution, which contained an estimated 200 mg of r-calbindin, was pumped through a 2.2 × 10 cm Pharmacia DEAE-Sephacel column packed in 10 mM Tris-HCl buffer at pH 7.5. The protein adhering to the column was eluted by means of a linear salt gradient (~1000 mL of solution in total) obtained by gradually mixing a 500-mL 10 mM Tris-HCl solution (pH 7.5) with an equal volume of the same solution but with 0.3 M NaCl added. Pumping speed was 50 mL/h, and 7-mL fractions were collected. The elution profile is shown in Figure 2.

Homogeneous 20% SDS–PAGE and IEF (pH 4.0–6.5) gels were obtained with prefabricated electrophoresis plates (Pharmacia) in a Pharmacia Phast System using the standard conditions recommended by the manufacturer. Visualization was by normal silver staining.

Purified fragments of the M2 mutant r-calbindin, obtained after limited digestion by trypsin, were sequenced by automated Edman degradation with a gas-phase sequencer (Applied Biosystems Model 470A, Foster City, CA) coupled to an in-line PTH amino acid analyzer (Applied Biosystems Model 120A).

NMR Spectroscopy. NMR samples of approximately 18 mg of wild-type r-calbindin were dissolved in 0.42 mL of H_2O/5% ^2H_2O. The pH was adjusted to 6.0 by addition of microliter amounts of 0.01 M NaOH or HCl. All spectra were acquired at 300K on Bruker AM500 spectrometers equipped with Aspect 3000 computers and digital phase shifting hardware. Raw data were processed on either an Aspect 3000 data station or a SUN 3/160C computer equipped with a SKY Warrior array processor. The software for the latter was a version of FTNMR provided by Dr. Dennis Hare and modified for use on the SUN by Dr. James Sayre.

Standard pulse sequences and phase cycling were utilized to acquire phase-sensitive COSY (Aue et al., 1976; Martin & Wüthrich, 1983), relayed-COSY, and double relayed-COSY (Wagner, 1983) spectra. A pure absorption NOESY spectrum with a 200-ms mixing period was acquired by using the normal pulse sequence (Macura & Ernst, 1980) followed by a short Hahn-echo period to improve the quality of the base line (M. Rance, unpublished results). In all spectra, quadrature phase detection in the ω_1 dimension was achieved by

[1] Abbreviations: NMR, nuclear magnetic resonance; COSY, correlated spectroscopy; DR-COSY, double relayed-COSY; 1(2)D, one-(two-)dimensional; NOE, nuclear Overhauser effect; NOESY, 2D NOE spectroscopy; IEF, isoelectric focusing; DEAE, diethylaminoethyl; r-calbindin, recombinantly expressed minor A bovine calbindin D_{9k}; EDTA, ethylenediaminetetraacetic acid; Tris, tris(hydroxymethyl)aminomethane.

[2] Recombinantly expressed calbindin D_{9k} has the sequence of the minor A form of the native protein with an extra N-terminal methionine residue designated Met0.

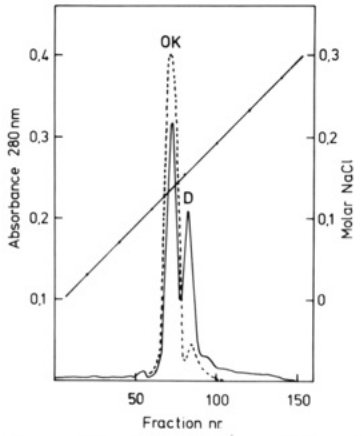

FIGURE 2: Elution profiles (absorbance at 280 nm) of r-calbindin fractions from a Pharmacia DEAE-Sephacel ion-exchange column. The solid line represents a preparation using a urea denaturation step, and the dashed line is for a preparation using heat treatment.

using time-proportional phase incrementation (Marion & Wüthrich, 1983). For each t_1 value, 2048 quadrature points were acquired for a spectral width of 6400 Hz. For COSY, relayed-COSY (τ = 40 ms), and double relayed-COSY (τ_1 = 22 ms, τ_2 = 38 ms) the spectral width in ω_1 was 4650 Hz, and 750, 450, and 350, respectively, t_1 values were collected. For NOESY the spectral width in ω_1 was 6000 Hz, and 450 t_1 values were collected. The COSY, relayed-COSY, and double relayed-COSY data were processed with pure sine bell weighting functions in the ω_2 dimension and $\pi/16$ to $\pi/64$ shifted sine bell weighting functions in the ω_1 dimension. The NOESY data were processed with $\pi/4$ to $\pi/12$ shifted sine bell weighting functions in the ω_2 dimension, followed by two-point spline function base-line correction after Fourier transformation. The spectrum of the first t_1 value was divided in half (Otting et al., 1986), then the ω_1 free induction decays were multiplied by $\pi/4$ shifted sine bell weighting functions and Fourier transformed. Backbone NH/C$^\alpha$H scalar coupling constants were measured as described by Marion and Wüthrich (1983).

Results

Isolation of the Different Isoforms of r-Calbindin. As mentioned above, IEF characterization of some wild-type and mutant r-calbindin preparations shows the presence of more than a single form of the protein. To separate the various isoforms, the isolation procedure was followed up to the Sephadex G-50 superfine column as previously described (Brodin et al., 1986). Thereafter, the solution was passed through a DEAE-Sephacel ion-exchange column. The proteins were eluted by using a slowly increasing salt gradient. The resulting elution profile (Absorbance at 280 nm) is shown in Figure 2. The migration pattern on SDS–PAGE and IEF gels of the r-calbindin from the DEAE-Sephacel fractions labeled OK and D and from other steps in the purification procedure is shown in Figure 3. The SDS–PAGE gels show that the r-calbindin fraction is homogeneous in size, but the IEF method clearly shows that fractions OK and D have different net charge. In addition, the former corresponds to a single isoform and the latter to two isoforms. Note that r-calbindin isoforms are not present in solution after the DEAE-cellulose column (lane 2 of Figure 3B), but are present after the Sephadex G-50 column (lane 3 of Figure 3B). The IEF gel also shows that a homogeneous r-calbindin fraction corresponding to the isoform with the lowest net charge (fraction OK) is obtained after the DEAE-Sephacel column (lane 4 of Figure 3B).

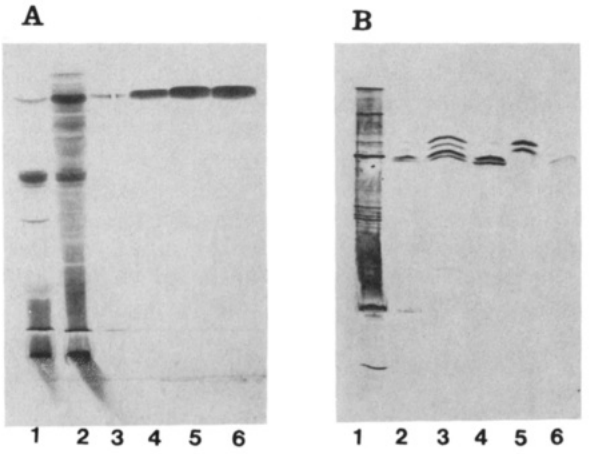

FIGURE 3: Homogeneous 20% SDS–PAGE (A) and isoelectric focusing [pH 4.0 (top)–6.5 (bottom)] electrophoresis (B) of r-calbindin fractions from different steps in the original purification procedure (Brodin et al., 1986; Linse et al., 1987). Equipment and conditions are described under Materials and Methods. The different lanes represent fractions from various steps in the original purification procedure: (1) soluble fraction obtained after the initial sonication of dispersed *E. coli* pellets; (2) pooled r-calbindin fractions obtained after passage of the sonicated sample through a DEAE-cellulose column; (3) r-calbindin fraction obtained after passage through a Sephadex G-50 column; (4) and (5) fractions labeled "OK" and "D", respectively (cf. Figure 2) in the eluate from the Pharmacia Sephacel column; (6) standard sample of wild-type r-calbindin used as internal reference.

Modification of the Purification Procedure To Prevent Formation of r-Calbindin Isoforms. On the basis of the gel results in Figure 3, we were led to suspect that r-calbindin isoforms appear as a result of deamidation of the protein when it is denatured in 8 M urea (Brodin et al., 1986). Since the objective of the urea treatment is removal of a low molecular weight contaminant that is tightly bound to the protein, this step was replaced by rapid thermal denaturation as follows. After the initial sonification, the ice-cold protein solution is poured into an equal volume of boiling buffer. The temperature of the protein solution is then raised from the resulting 55 ± 5 to 95 °C in 2 min or less, followed immediately by rapid cooling on ice. This procedure effectively releases the contaminant and causes practically no deamidation (Figures 2 and 4). SDS–PAGE and IEF gels show that a homogeneous r-calbindin fraction corresponding to the intact protein is obtained after the Sephadex G-50 column (lanes 5 of Figure 4). Note that in this new procedure the denaturation step is carried out *before* the DEAE-cellulose column.

Characterization of the Isoforms by Protein Sequencing. Amino acid sequencing of the protein was carried out in an attempt to establish the differences between the various isoforms. For this particular analysis, a preparation of the M2 mutant r-calbindin (Pro20→Gly + ΔAsn21; Linse et al., 1987) was used rather than wild-type protein, because approximately equimolar amounts of OK and D forms were obtained. This sample was initially treated with trypsin, which produces one major cleavage product. While homogeneous on SDS gels, IEF revealed the presence of two isoforms with differing net charge. The two isoforms were separated on a DEAE-Sephacel column and are hereafter denoted fragments A and B. The amino acid analyses of the two fragments indicate that they represent residues 42–71 of wild-type r-calbindin. The sequence of fragment B was identical with that of fragment A except that Asn56 is converted to Asp56, with only a trace of Asn at that position in fragment B. Deamidation at this specific site had in fact been suspected, since this is the only site in the protein with the Asn-Gly dipeptide that is known

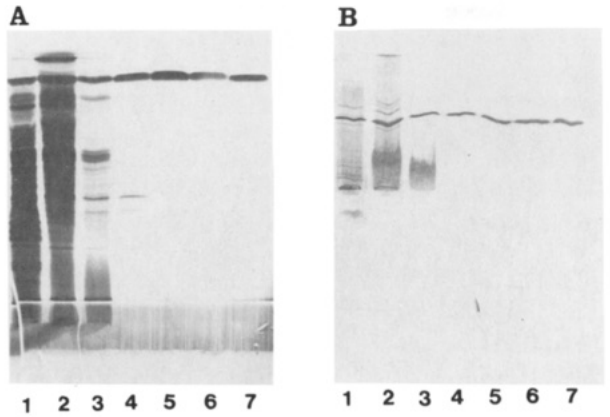

FIGURE 4: Homogeneous 20% SDS–PAGE (A) and isoelectric focusing [pH 4.0 (top)–6.5 (bottom)] electrophoresis (B) of r-calbindin fractions from different stages in the modified purification procedure wherein urea denaturation is replaced by thermal denaturation as described in the text. Equipment and conditions were identical with those in Figure 3 and are described under Materials and Methods. In general, the differences observed in background staining with respect to gels shown in Figure 3 are the result of differences in development time for the silver staining. The different lanes represent fractions from the following successive steps in the new purification procedure: (1) soluble fraction obtained after sonication of *E. coli* pellets; (2) supernatant obtained after the rapid thermal denaturation step as outlined in text; (3) dialyzed supernatant obtained after precipitation with ammonium sulfate, 0.45 g/mL; (4) r-calbindin fraction obtained after passage through the DEAE-cellulose column; (5) r-calbindin fraction obtained after passage through the Sephadex G-50 column; (6) r-calbindin fraction OK eluted by a linear salt gradient from the DEAE-Sephacel column (cf. Figure 2); (7) reference sample of wild-type r-calbindin.

to have a high propensity for deamidation.

Every residue, except the C-terminal lysine, was identified in each fragment. A repetitive yield (average of two determinations) of 89% was obtained for the sequencing of the whole of fragment A. While a similar repetitive yield of 92% was obtained for the Gly42–Lys55 portion of fragment B, there was a sharp drop to less than 20% between Lys55 and Asn56. The repetitive yield for the following residues was only 70%. On the basis of the fact that isopeptide bonds are not cleaved during Edman degradation (Groskopf et al., 1966; Weber & Konigsberg, 1967), these results strongly suggest that deamidation was accompanied by approximately 80% isomerization to an isoaspartyl–gycine sequence. This hypothesis has been substantiated by 2D ^{1}H NMR.

Analysis of Structure Using 2D ^{1}H NMR. The key element in any detailed analysis by ^{1}H NMR is the assignment of resonances to specific hydrogen atoms in the molecule (sequence-specific assignment). The basic approach is to identify the ^{1}H spin systems for each amino acid via scalar (through-bond) coupling and then to assign each spin system to the appropriate location in the sequence from the characteristic nuclear Overhauser effects (through-space couplings) between backbone amide, C^α, and side-chain protons of residues that are adjacent in the sequence [reviewed in Wüthrich (1986)]. The starting point for the studies reported here is the complete sequence-specific assignment of the ^{1}H NMR spectrum of purified intact r-calbindin (Chazin et al., 1989; Kördel et al., 1989).[3]

[3] Conformational heterogeneity arising from cis–trans isomerism at Pro43 (Chazin et al., 1989) is observed in both the intact and the deamidated forms of the protein. For technical reasons and to facilitate discussion, in this comparative study we concentrate on the significantly more abundant *trans*-Pro43 forms.

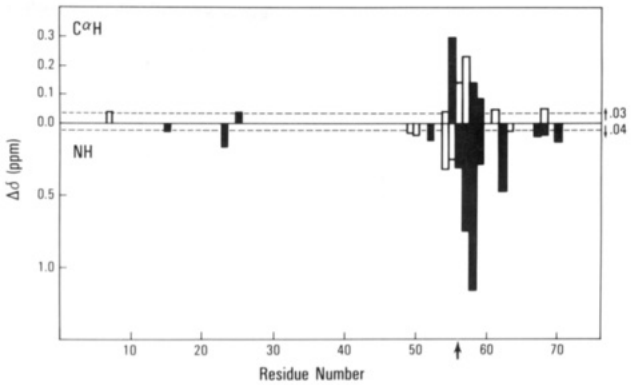

FIGURE 5: Backbone chemical shift differences between intact r-calbindin (Asn56) and the β-linked (isoaspartyl) product of deamidation. Solid bars represent upfield shifts and open bars downfield shifts. The experimental error in these numbers is ±0.02 ppm. The dashed lines indicate the lower limit for consideration of chemical shift differences as significant.

The assignment of the deamidated forms of r-calbindin was greatly facilitated by the fact that not only the backbone proton chemical shifts but also the side-chain chemical shifts of many of the residues are essentially identical with those in the intact protein. In parallel to an earlier study of a chemically modified protein (Chazin et al., 1985), a large percentage of the assignments could be made by simple comparison of corresponding cross peaks in 2D spectra obtained under identical conditions. The observation of relayed connectivities in the DR-COSY spectrum from the side-chain protons to the backbone amide proton proved to be extremely useful for obtaining these "assignments by comparison" in an efficient manner. This left only a small subset of cross peaks to be examined in detail. The assignment of the unique resonances of the major and minor deamidated isoforms is discussed below.

For the major isoform, significant differences in chemical shifts relative to the intact protein are observed almost exclusively in the C-terminal Ca^{2+}-binding loop (Asp54–Glu65) as shown in Figure 5. The in-depth ^{1}H NMR analysis of this polypeptide segment was originated at the characteristic low field shifted amide proton resonance of Gly59, which has a chemical shift of 10.49 ppm in the intact protein. While there is a substantial difference in the amide chemical shift observed for the major deamidated form (10.76 ppm), the uniqueness of the amide proton shift and the observation of two C^α shifts that are very similar to those of the intact protein are sufficient evidence for assuming that the assignment can be transferred. This sequence-specific assignment was verified and extended to the other residues in the Asp54–Glu 65 loop by the sequential assignment procedure.

In the polypeptide segment Asp54–Glu65, sequence-specific assignments could be made via observation of strong $d_{\alpha N}(i, i+1)$ connectivities for Asp54–Lys55, Gly57–Asp58, and Glu60–Ser62 and strong $d_{NN}(i, i+1)$ connectivities for Asp58–Glu60 and Ser62–Glu65. In each case, the C^αH resonance was identified by the C^αH/NH COSY cross peak, and the corresponding side-chain assignments were obtained from the COSY and DR-COSY spectra. Figures 6 and 7 show selected regions of a DR-COSY spectrum and a NOESY spectrum (τ_m = 200 ms) acquired from a solution containing a mixture of the two isoforms of r-calbindin. Resonances are identified for residues (of both the major and minor isoforms) in the polypeptide segment Asp54–Val61. A third set of resonances corresponding to the <5% of intact protein present in the mixture is also observed in the ^{1}H spectrum, but the corresponding cross peaks are extremely weak.

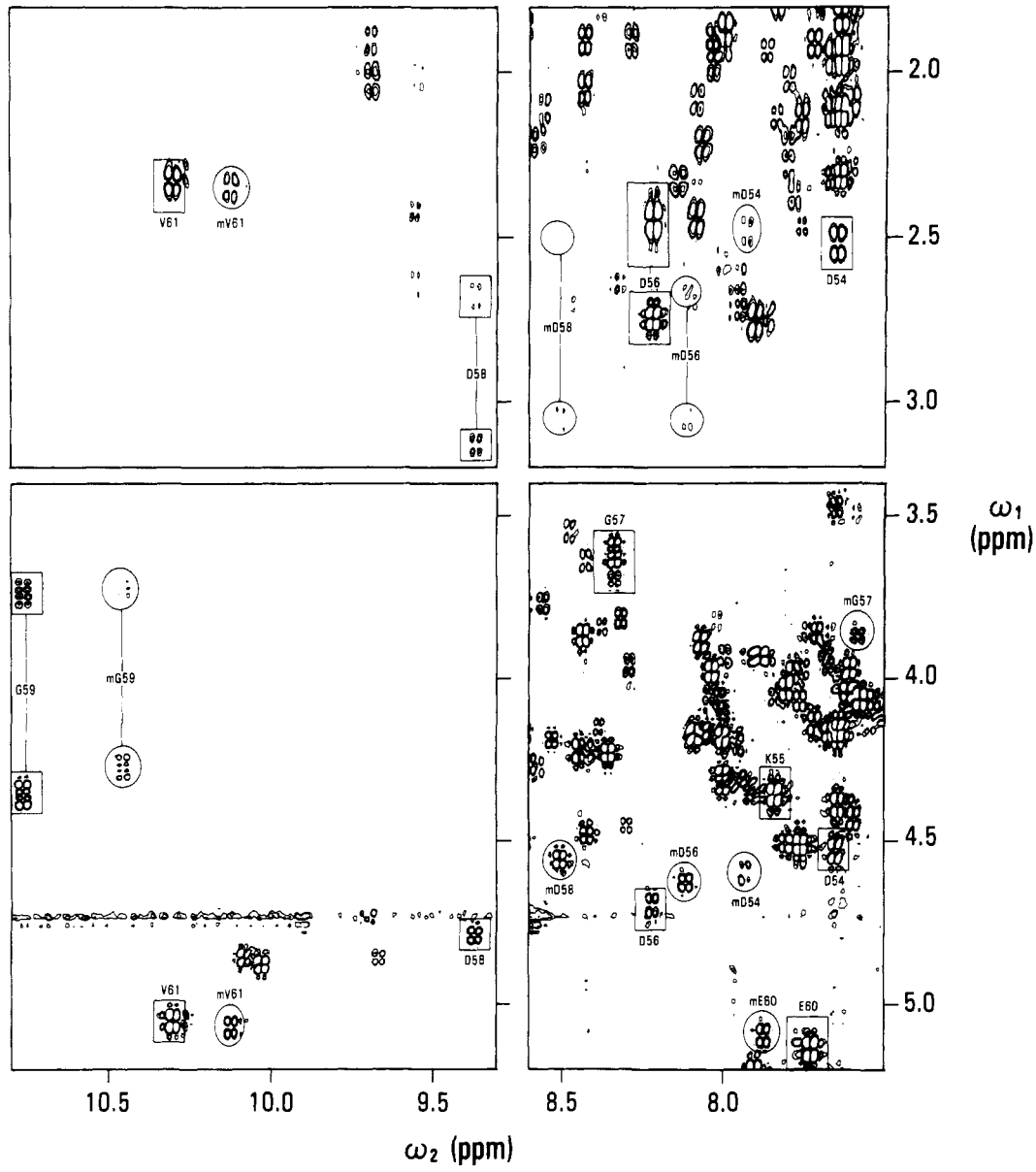

FIGURE 6: Regions of a 500-MHz double relayed-COSY spectrum of deamidated r-calbindin acquired at 300 K from a 4 mM self-buffered solution at pH 6.0. The lower panel contains $\omega_1 = C^{\alpha}H$, $\omega_2 = NH$ cross peaks, and the upper panel contains $\omega_1 = C^{\beta}H$, $\omega_2 = NH$ cross peaks. A selected number of cross peaks arising from residues near the site of deamidation (Asn56) are labeled with the sequence-specific assignment. Resonances from the major deamidated isoform are boxed; those from the minor isoform (m) are circled.

The key data for sequence-specific assignments have been summarized above for all residues up to Lys55 and from Gly57, leaving only a gap at residue 56. Two strong sequential connectivities at 2.43 and 2.73 ppm are observed in the NOESY spectrum at the amide proton resonance frequency of Gly57 (Figure 7). These are assigned to the C^{β} protons of the preceding residue, the putative Asn→Asp56. Starting with the $C^{\beta}H$ assignments, the $C^{\alpha}H$ and backbone NH resonances of this spin system could be identified by tracing the $C^{\beta}H/C^{\beta'}H$, $C^{\beta}H/C^{\alpha}H$ and $C^{\alpha}H/NH$ cross peaks in the COSY spectrum and from relayed connectivities in the DR-COSY spectrum (Figure 6). The strong sequential NOE at the backbone NH resonance of residue 56 from the C^{α} proton of Lys55 (Figure 7) provides the final sequential connectivity. The data therefore lead to an unambiguous assignment of resonances for residue 56 and provide complete sequence-specific assignments of the ^1H NMR spectrum of the major isoform.

Two lines of evidence from the ^1H NMR data strongly imply that the most abundant species in the mixture (the major isoform) is a product of deamidation of the native protein. First, there are extraordinarily large changes in the two C^{β} proton chemical shifts relative to Asn56 in the intact protein ($\Delta\delta = -0.43, -0.57$ ppm), indicative of a substantial chemical and/or structural perturbation at C^{β} of this residue. Second, one set of side-chain amide resonances was clearly absent from the ^1H spectrum, those of Asn 56. The ^1H NMR analysis and amino acid sequencing are therefore in agreement that the protein is deamidated at Asn56.

With the major isoform identified as the Asn56→Asp protein, there remained a question as to the origin of the minor isoform. The protocol utilized to assign the resonances of the major isoform was repeated for the resonances of the second most abundant species in solution. There is in fact a much closer correspondence between the intact protein and this minor isoform than for the major isoform. While this greatly facilitated the assignment process, the similarity of the two meant that careful analysis was required to establish any differences between them. The only truly significant difference in any of the chemical shifts relative to the native protein was for

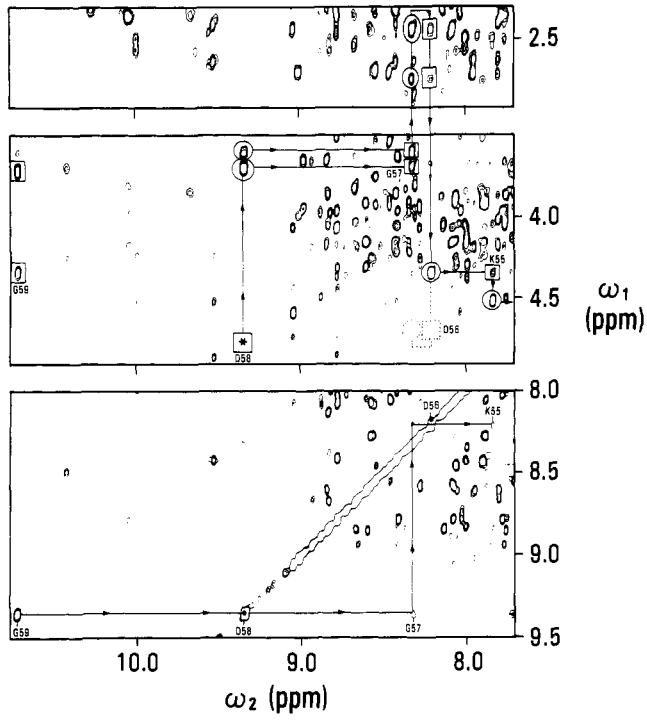

FIGURE 7: Paths of sequential NOE connectivities for the major form of deamidated calbindin D_{9k}. Regions of a 500-MHz Hahn-echo NOESY spectrum of deamidated r-calbindin acquired with a 200-ms mixing period at 300 K from a 4 mM self-buffered solution at pH 6.0 are shown. Cross peaks indicating short distances between $C^{\beta}H$ (upper panel), $C^{\alpha}H$ (middle panel), and backbone NH (lower panel) resonances and a backbone NH resonance of a sequentially adjacent residue are highlighted. The pathway of connectivities for the polypeptide segment Asp54–Gly59 is identified with a solid line, and cross peaks are labeled with the sequence-specific assignment. The star indicates that the $C^{\alpha}H$ resonance of Asp58 is saturated at this temperature due to irradiation of the H_2O signal. The dashed box and dashed circle indicate the location of the intraresidue and interresidue $d_{\alpha N}$ cross peaks, respectively, which can only be observed at very low contour levels.[4]

residue 56. As for the major isoform, both the absence of Asn56 side chain amide resonances and the large upfield shifts of the C^{β} protons ($\Delta\delta$ = −0.24, −0.26 ppm) imply that the minor isoform is also the product of deamidation at Asn56. The presence of two isoforms as a result of deamidation of a single site can be readily explained, as indicated in Figure 1. Since there is a closer correspondence of chemical shifts and observed NOEs to the intact protein, the minor isoform was assigned as the isomer with a normal α-peptide linkage.

To establish the nature of the Asp56-Gly57 peptide linkage of the major isoform, an extensive effort was made to carefully characterize the sequential NOEs. In the NOESY spectrum acquired with a 200-ms mixing period, the $d_{\beta N}$ connectivities are strong, but both the $d_{\alpha N}$ and d_{NN} connectivities are extremely weak[4] (Figure 7). Since there is no experimental evidence for anomalous correlation times (enhanced mobility or conformational heterogeneity on a rapid time scale) in this region of the molecule, the low intensities indicate that the interproton distances are near the upper limits observable at this mixing time. On the basis of considerations of spin diffusion, comparison to extensive studies of NOE buildup for intact r-calbindin (Kördel, Forsén, and Chazin, unpublished results), and internal comparisons to NOEs between other adjacent backbone protons observed in this spectrum, the $d_{\alpha N}$ and d_{NN} interproton distances must fall in the range 4–6 Å. Such an observation is inconsistent with a normal α-linked peptide backbone because structural constraints force at least one of the two distances ($d_{\alpha N}$, d_{NN}) to be less than 3 Å (Billeter et al., 1982). In a β-linked peptide, it is the $d_{\beta N}$ distances that are structurally constrained to be always less than 3.5 Å (in analogy to the $d_{\alpha N}$ distances for an α-linked peptide backbone), whereas the upper limits on the $d_{\alpha N}$ and d_{NN} distances are considerably higher (approximately 4.7 and 6.0 Å, respectively) because there is an extra carbon atom in the main chain of the polypeptide (Figure 1). The intensities of the d_{NN}, $d_{\alpha N}$, and $d_{\beta N}$ NOEs observed for the major isoform are therefore fully consistent with the presence of a β-linked peptide bond between residues (iso-)Asp56 and Gly57. We note that the positive identification of the major isoform as the β-linked isomer is in agreement with the amino acid sequencing analysis and with the identification of the minor species as an α-linked isoform.

The side-chain carbonyl of Asn56 is a Ca^{2+} ligand in site II, and deamidation is accompanied by measurable changes in the Ca^{2+} affinity (S. Linse, T. Drakenberg, E. Thulin, S. Forsén, unpublished experiments).[5] It was therefore deemed important to characterize any differences in global or local conformation between the intact and deamidated forms of the protein. We have carefully examined the following parameters: chemical shifts of the backbone NH, $C^{\alpha}H$, $C^{\beta}H$, methyl, and aromatic protons, the ϕ backbone dihedral angles as determined from $^3J_{HN\alpha}$, and the occurrence and intensity of sequential d_{NN} and $d_{\alpha N}$ NOEs. In both deamidated forms, significant chemical shift differences relative to the intact protein were found only in the region near residue 56. Significant differences (>1 Hz) in $^3J_{HN\alpha}$ were observed only for Asp54, Lys55, and Asn→Asp56 and only in the β-linked isoform. In each case, higher values were found relative to the intact protein (8.1 vs 6.4 Hz, 8.2 vs 5.7, 10.4 vs 9.4 Hz, respectively). A comparative analysis of the sequential NOE connectivities also showed significant differences in NOEs only for the β-isoform and exclusively in the polypeptide segment Lys55–Asp58. In a spectrum acquired with a 200-ms mixing time, the intact protein and α-linked isoform exhibit strong d_{NN} and weak $d_{\alpha N}$ conectivities throughout this segment. For the β-linked isoform the connectivities are as follows: strong $d_{\alpha N}$ and no d_{NN} from Lys55 to iso-Asp56; strong $d_{\beta N}$ and weak $d_{\alpha N}$ and d_{NN} from iso-Asp56 to Gly57; strong $d_{\alpha N}$ and weak d_{NN} connectivity from Gly57 to Asp58. The NOE and coupling constant data indicate a general tendency of change from helical-type backbone conformation in the intact and α-linked deamidated proteins to a more extended conformation in the β-linked isoform. The cumulative effect corresponds to a local expansion of the loop in this region. Although a significant change in the conformation of this polypeptide segment in the β-linked isoform is clearly indicated, the data presently available are not sufficiently accurate or complete to provide a detailed description of the changes in tertiary structure produced by isopeptide formation. These differences and their

[4] A referee has suggested that the low intensities of the $d_{N\alpha}$ and $d_{\alpha N}$ connectivities of iso-Asp56 in the NOESY spectrum of Figure 7 may be due to the close proximity of the $C^{\alpha}H$ resonance to the H_2O saturation frequency. The small size of these NOEs has been verified in a NOESY experiment wherein H_2O suppression is obtained without saturation by replacing the observe pulse with a $90°_x$–τ–$90°_{-x}$ selective excitation sequence (Plateau & Guéron, 1982).

[5] The macroscopic Ca^{2+} binding constants (K_1, K_2) for intact r-calbindin are 1.6×10^8 and 4.0×10^8 M^{-1}. Slightly higher values (2.5×10^8 and 6.3×10^8 M^{-1}) are observed for the α-linked form, probably due to the increased charge in site II. Significantly lower values (2.0×10^7 and 3.2×10^7 M^{-1}) are observed for the β-linked form, which we assume are the result of structural perturbations.

relation to effects on calcium binding will be explored in more detail by obtaining additional data to carefully determine distance and dihedral angle constraints for calculations of the three-dimensional structure.

Discussion

The possibility that deamidation and the formation of isopeptide linkages could affect the physiological properties of protein molecules should be of some concern in the biomedical field. Unwanted deamidation of mammalian proteins, expressed in microorganisms and intended for human medical or veterinary use, may result in undesirable and unacceptable immunological responses or pyrogenic effects. There is a need for methods to rapidly and unambiguously identify such sites of protein modification. Deamidation of Asn and Gln residues at unspecified sites may be relatively easily detected by analytical techniques that are sensitive to changes in total charge or isoelectric point. The determination of the specific amino acid residues involved may be accomplished through protein sequencing. On the other hand, the unambiguous identification by bioanalytical techniques of isopeptide linkages, typically isoaspartate, is considerably more difficult, and a very limited number of such studies have been carried out on proteins (DiDonato et al., 1986; Aswad et al., 1988; Johnson et al., 1987). Indirect evidence for such linkages has, however, been obtained, for example, through the observed failure to sequence a protein beyond a certain amino acid. This is because cyclization and cleavage of the thiocarbamyl peptide to the thiazolidone amino acid does not occur during Edman degradation when the amino terminal is an isopeptide linkage (Groskopf et al., 1966; Weber & Konigsberg, 1967). The 2D ^{1}H NMR methods described herein represent a novel and nondestructive approach to the identification of isoaspartyl residues in proteins and should be generally applicable in all cases where 2D ^{1}H NMR spectra of good quality can be obtained and when sequence-specific assignments can be established.

In this paper, we describe the isolation, purification, and characterization of three isoforms of r-calbindin. We note that similar deamidated forms of native protein preparations have been observed in samples kept at neutral pH for several months. Detailed structural analysis of the deamidated forms of the protein by 2D ^{1}H NMR has demonstrated the existence of a β-linked isomer and a 4:1 preference for this form over the α-linked isomer. Interestingly, model studies on peptides have generally shown a 4:1 preference for the β-linked peptide (Aswad & Johnson, 1987; McFadden & Clarke, 1987; Meinwald et al., 1986). This suggests that the three-dimensional structure of calbindin D_{9k} does not play a key role in determining the relative rates by which the intermediate five-membered imide ring is opened to form the α- or β-peptide linkage (cf. Figure 1).

It was recently shown by Kossiakoff that neutron diffraction studies at high resolution allow the identification of specific deamidation sites in crystalline trypsin (Kossiakoff, 1988). In this particular protein all three observed deamidated groups have the sequence X-Asn-Ser, and no isopeptide linkage was observed. As was also noted by Kossiakoff, isopeptide linkages should be readily distinguishable in X-ray diffraction studies of crystalline proteins. The total absence of such findings in the X-ray crystallographic literature was attributed to the fact that this type of linkage has not been expected and therefore overlooked during model building. It is also possible that the Asn–Gly peptide bonds are only partially modified, resulting in a mixture of structural species that causes statistical disorder in the crystal structure.

In high-resolution 2D NMR studies of proteins, the presence of multiple forms in solution is often readily identifiable. Both conformational (Chazin et al., 1989) and now chemical heterogeneity have been found in bovine calbindin D_{9k}. Through in-depth analysis of a variety of NMR parameters, it is possible to characterize the extent of differences between various forms of the protein. Sequence-specific assignments provide the opportunity to identify the site(s) of perturbation. In this study, the chemical shift, coupling constant, and NOE data taken together show that the global conformation of bovine calbindin D_{9k} is not perturbed upon deamidation, that all elements of secondary structure are intact, and that in the β-linked isoform there is a highly localized perturbation of the protein conformation near the site of deamidation with significant effects only over the polypeptide segment Lys55–Asp58.

Acknowledgments

We thank Dr. Mark Rance for continued support with experimental methods, Dr. Thomas Grundström and Peter Brodin for supplying the protein pellets isolated from *E. coli*, Kathy Carpenter for assistance in preparation of the manuscript, and referees for their helpful comments and suggestions.

References

Ahern T. J., & Klibanov, A. M. (1987) *Methods Biochem. Anal. 33*, 91–127.

Aswad, D. W., & Johnson, B. A. (1987) *Trends Biochem. Sci. 12*, 155–158.

Aswad, D. W., Gleason, C. S., & Miller, P. G. (1988) *FASEB J. 2*, A555.

Aue, W. P., Batholdi, E., & Ernst, R. R. (1976) *J. Chem. Phys. 64*, 2229–2246.

Billeter, M., Braun, W., & Wüthrich, K. (1982) *J. Mol. Biol. 155*, 321–346.

Bornstein, P. (1970) *Biochemistry 9*, 2408–2421.

Bornstein, P., & Balian, G. (1970) *J. Biol. Chem. 245*, 4854–4856.

Brodin, P., Grundström, T., Hofmann, T., Drakenberg, T., Thulin, E., & Forsén S. (1986) *Biochemistry 25*, 5371–5377.

Chazin, W. J., Goldenberg, D. P., Creighton, T. E., & Wüthrich, K. (1985) *Eur. J. Biochem. 152*, 429–437.

Chazin, W. J., Kördel, J., Drakenberg, T., Thulin, E., Brodin, P., Grundström, T., & Forsén, S. (1989) *Proc. Natl. Acad. Sci. U.S.A. 86*, 2195–2198.

Clarke, S. (1985) *Annu. Rev. Biochem. 54*, 479–506.

DiAugustine, R. P., Gibson, B. W., Aberth, W., Kelly, M., Ferrua, C. M., Tomooka, Y., Brown, C. F., & Walker, M. (1987) *Anal. Biochem. 165*, 420–429.

DiDonato, A., Galletti, P., & D'Alessio, G. (1986) *Biochemistry 25*, 8361–8368.

Geiger, T., & Clarke, S. (1987) *J. Biol. Chem. 262*, 785–794.

Gracy, R. W. (1983) in *Current Topics in Biological and Medical Research* (Rattazzi, M. C., Scandalios, J. G., & Witt, G. S., Eds.) Vol. 7, pp 187–201, Liss, New York.

Groskopf, W. R., Holleman, J. W., Margoliash, E., & Klotz, I. M. (1966) *Biochemistry 5*, 3783–3796.

Harding, J. J. (1985) *Adv. Protein Chem. 37*, 247–334.

Ikeda, A., & Sawano, J. (1971) *Acta Soc. Ophthalmol. Jpn. 75*, 1277–1283.

Johnson, B. A., Langmark, E. L., & Aswad, D. W. (1987) *J. Biol. Chem. 262*, 12283–12287.

Kördel, J., Forsén, S., & Chazin, W. J. (1989) *Biochemistry 28*, 7065–7074.

Kossiakoff, A. A. (1988) *Science 240*, 191–194.

Linse, S., Brodin, P., Drakenberg, T., Thulin, E., Sellers, P., Elmden, K., Grundström, T., & Forsén, S. (1987) *Biochemistry 26*, 6723-6735.
Macura, S., & Ernst, R. R. (1980) *Mol. Phys. 41*, 95-117.
Marion, D., & Wüthrich, K. (1983) *Biochem. Biophys. Res. Commun. 113*, 967-974.
McFadden, P. N., & Clarke, S. (1987) *Proc. Natl. Acad. Sci. U.S.A. 84*, 2595-2599.
Meinwald, Y. C., Stimson, E. R., & Scheraga, H. A. (1986) *Int. J. Pept. Res. 28*, 79-84.
Otting, G., Widmer, H., Wagner, G., & Wüthrich, K. (1986) *J. Magn. Reson. 66*, 197-193.
Plateau, P., & Guêron, M. (1982) *J. Am. Chem. Soc. 104*, 7310-7311.
Robinson, A. B. (1979) *Mech. Aging Dev. 9*, 225-236.
Robinson, A. B., & Rudd, C. J. (1987) in *Current Topics in Cellular Regulation* (Horecker, B. L., & Stadtman, E. R., Eds.) pp 247-295, Academic Press, New York.
Tollefsbol, T. O., & Gracy, R. W. (1983) *BioScience 33*, 634-639.
Turner, B. M., Fisher, R. A., & Harris, H. (1975) in *Isozymes* (Markert, C. L., Ed.) Vol. 1, pp 781-795, Academic Press, New York.
Wagner, G. (1983) *J. Magn. Reson. 55*, 151-156.
Weber, K. L., & Konigsberg, W. (1967) *J. Biol. Chem. 242*, 3563-3578.
Wüthrich, K. (1986) *NMR of Proteins and Nucleic Acids*, Wiley, New York.
Yüksel, K. Ü., & Gracy, R. W. (1986) *Arch. Biochem. Biophys. 248*, 452-459.

Free Radicals Induced by Adriamycin-Sensitive and Adriamycin-Resistant Cells: A Spin-Trapping Study†

A. E. Alegria,‡ A. Samuni,§ J. B. Mitchell,‡ P. Riesz,‡ and A. Russo*,‡

Radiation Oncology Branch, Clinical Oncology Program, Division of Cancer Treatment, National Cancer Institute, National Institutes of Health, Building 10, Room B3-B69, Bethesda, Maryland 20892, and Molecular Biology, School of Medicine, Hebrew University, Jerusalem 91010, Israel

Received February 14, 1989; Revised Manuscript Received April 28, 1989

ABSTRACT: The radicals generated by adriamycin-sensitive (CHO-AB) and adriamycin-resistant (CHO-C5) Chinese hamster ovary cells as well as by adriamycin-sensitive and -resistant human breast cancer cells (MCF7-WT and MCF7-ADR) have been studied with spin-trapping and ESR spectroscopy. During anoxic exposure to adriamycin (ADR) both pairs of cell lines produced the broad ESR singlet characteristic of ADR semiquinone ($AQ^{\bullet}$). By use of tris(oxalato)chromate (CrOx) as an extracellular line-broadening agent, the distribution of $AQ^{\bullet}$ between the intra- and extracellular compartments was studied. For cell densities of $(1-3) \times 10^7$ cells/mL, CrOx eliminated most, though not all, of the ESR signal, indicating that the $AQ^{\bullet}$ radicals freely diffuse and partition between the intra- and extracellular compartments proportionally to their respective volumes. Similar behavior was exhibited by all four cell lines studied. Upon introduction of oxygen to anoxic cells in the presence of the spin trap 5,5-dimethylpyrroline *N*-oxide (DMPO), the $AQ^{\bullet}$ signal was replaced by that of the DMPO–OH spin adduct. Metal chelators such as desferrioxamine had no effect on DMPO–OH or $AQ^{\bullet}$ formation. Superoxide dismutase, not catalase, totally eliminated the ESR signal, indicating that DMPO–OH produced by ADR-treated cells originates from superoxide rather than from $^{\bullet}OH$ produced from H_2O_2. In the presence of CrOx, the DMPO–OH signal was not distinguishable from the background noise, thus excluding any contribution to the signal by intracellular spin adducts. Without excluding a possible role for intracellular $O_2^{\bullet-}$ and $^{\bullet}OH$ radicals, the present results show that $AQ^{\bullet}$ radicals partition predominantly outside the cell and react there with oxygen to yield extracellular superoxide. Since ADR-resistant and -sensitive cell lines generated comparable levels of the radicals, there is little support for the assumption that ESR-observable oxygen-derived radicals play a role in ADR antitumor activity.

The anthracycline antibiotics, which include adriamycin (ADR),[1] possess significant therapeutic activity against most hematologic, lung, breast, and ovarian malignancies; however, their clinical use is restricted by cumulative dose-dependent cardiotoxicity. Were the chemical and biological mechanisms of action of ADR more thoroughly defined, strategies could be instituted to improve the therapeutic index. Although ADR has been found to have multiple cellular targets, the cardiotoxicity and antitumor effects have been suggested to occur through different biochemical mechanisms. The proposed cardiotoxic mechanisms include production of ADR-mediated

† A.E.A. is grateful for the NIH-NIGMS MARC Program (Award 3-734-GM 12247) for supporting his sabbatical leave. This work was supported in part by a grant from the Israel-U.S. Binational Science Foundation.

* To whom correspondece should be addressed.
‡ National Institutes of Health.
§ Hebrew University.

[1] Abbreviations: ESR, electron spin resonance; DMPO, 5,5-dimethyl-1-pyrroline *N*-oxide; DTPA, diethylenetriaminepentaacetic acid; DFO, desferrioxamine; CrOx, tris(oxalato)chromate; CHO, Chinese hamster ovary cells; MCF7, human breast carcinoma cells; ADR, adriamycin; $AQ^{\bullet}$, adriamycin semiquinone free radical; GSH, glutathione; PBS, phosphate buffered saline.